An effective frequency-domain feature of atrial fibrillation based on time-frequency analysis

Yusong Hu
Northeastern University
Yantao Zhao
Northeastern University
Jihong Liu (liujihong@ise.neu.edu.cn)
Northeastern University https://orcid.org/0000-0002-0733-4746
Jin Pang
Northeastern University
Chen Zhang
Northeastern University
Peizhe Li
Northeastern University

Research article

Keywords: atrial fibrillation; frequency-domain feature; time-frequency analysis; ECG; decision tree algorithm

Posted Date: March 19th, 2020

DOI: https://doi.org/10.21203/rs.2.21462/v2

Version of Record: A version of this preprint was published on November 25th, 2020. See the published version at https://doi.org/10.1186/s12911-020-01337-1.

An effective frequency-domain feature of atrial fibrillation based on time-frequency analysis

Yusong Hu[+], Yantao Zhao[+], Jihong Liu*, Jin Pang, Chen Zhang, and Peizhe Li

College of Information Science and Engineering, Northeastern University, Shenyang, Liaoning, China

*Corresponding author: Jihong Liu (e-mail: liujihong@mail.neu.edu.cn, Orcid: 0000-0002-0733-4746)

[+]Joint first author

Yusong Hu, e-mail: 20174315@stu.neu.edu.cn,

Yantao Zhao, e-mail: 20173745@stu.neu.edu.cn

Jin Pang, e-mail: 20171716@stu.neu.edu.cn

Chen Zhang, e-mail: 20173346@stu.neu.edu.cn

Peizhe Li, e-mail: 20164098@stu.neu.edu.cn

An effective frequency-domain feature of atrial fibrillation based on time-frequency analysis

Abstract

Background: Atrial fibrillation is a type of persistent arrhythmia that can lead to serious complications. Therefore, accurate and quick detection of atrial fibrillation by surface electrocardiogram has great importance on further treatment. The practical electrocardiogram signals contain various interferences in different frequencies, such as myoelectricity interference, power interference and so on. Detection speed and accuracy largely depend on the atrial fibrillation signal features extracted by the algorithm. But some of the discovered atrial fibrillation features are not well distinguishable, resulting in poor classification effect.

Methods: This paper proposed a high distinguishable frequency feature - the frequency corresponding to the maximum amplitude in the frequency spectrum. We used the R-R interval detection method optimized with the mathematical morphology method and combined with the wavelet transform method for analysis. According to the two features - the maximum amplitude in the frequency spectrum and R-R interval irregular, we could recognize atrial fibrillation signals in electrocardiogram signals by decision tree classification algorithm.

Results: The data used in the experiment come from the MIT-BIH database, which is publicly accessible via the web and with ethical approval and consent. Based on the input of time-domain and frequency-domain features, we classified sinus rhythm signals and AF signals using the decision tree generated by classification and regression tree (CART) algorithm. From the confusion matrix, we got the accuracy was 98.9%, sensitivity was 97.93% and specificity was 99.63%.

Conclusions: The experimental results can prove the validity of the maximum amplitude in the frequency spectrum and the practicability and accuracy of the detection method, which applied this frequency-domain feature. Through the detection method, we obtained good accuracy of classifying sinus rhythm signals and atrial fibrillation signals. And the sensitivity and specificity of our method were pretty good by comparison with other studies.

Key words: atrial fibrillation; frequency-domain feature; time-frequency analysis; ECG; decision tree algorithm

I. BACKGROUND

Atrial fibrillation (AF) is the most common arrhythmia, with a prevalence rate of 1.5% to 2% in developed countries [1]. When AF occurs, the regular order of atrial electrical activity disappears, replaced by the fast and disorderly tremor waves, and the atrial electrical activity is seriously disordered. Patients with AF are often accompanied by symptoms such as palpitations, arrhythmia, shortness of breath, and chest pain. The incidence of AF increases with age, and the most serious complication is stroke. Early diagnosis can effectively reduce the incidence of complications caused by AF.

An electrocardiogram (ECG) is a technique that uses a medical device to collect and record a pattern of changes in activity produced by the heart. Compared with other bioelectrical signals, ECG signals are easier to be monitored and have morphological regularity. Typical ECG signals mainly include P wave, Q wave, R wave, S wave, and T wave, as shown in Figure 1. When AF occurs, the original normal P-waves disappear and are replaced by a series of irregular high-frequency oscillations called F-waves; the distance between R waves varies irregularly. The above two features have become the basis of the current automatic detection AF technology [2].

The current diagnosis of AF relies primarily on the presence of some typical symptoms of the patient and the characteristics of the ECG recording. However, early and accurate detection of AF remains a challenge. For asymptomatic paroxysmal AF, the detection of it needs about 72-hour ECG signals [3]. Therefore, it is valuable to develop an automatic detection algorithm that can diagnose AF quickly, accurately and reliably [2]. It is also of great significance to explore effective and high distinguishable features of atrial fibrillation to realize the automatic detection of atrial fibrillation.

Moody et al. proposed an automatic method for detecting atrial fibrillation based on the difference between the atrial fibrillation signal and the sinus rhythm signal in the RR interval [4]. Tateno et al. proposed a method based on the RR interval and coefficient [5]. And they identify the difference between sinus rhythm signal and AF signal by using the Kolmogorov-Smirnov test. These studies based on the RR interval achieved 97% accuracy of automatic detection. Using empirical mode decomposition, Uday Maji et al. found significant differences in the fourth layer intrinsic mode function (IMF4), with an accuracy of 96% [6].

Recently, some scholars have regarded AF as an abnormal phenomenon and analyzed it as a signal abnormality. Paolo Massimo Buscema et al. [7] proposed to apply an improved BP neural network for the diagnosis of AF. This method used a Supervised Contractive Map neural network structure and achieved the diagnosis of AF with an accuracy rate of 95%. He Runnan et al. [8] proposed a way of detecting AF based on Continues Wavelet Transform(CWT) and two-dimensional convolutional neural network by analyzing ECG's overall time-frequency features. S. Asgari et al. [9] applied wavelet transform to extract peak-to-average power ratio and logarithmic energy entropy as feature vectors for AF detection.

Common methods to extract F wave include the QRST cancellation method, ICA analysis method based on principal component analysis, etc. The QRST cancellation method is very sensitive to the change of waveform and greatly depends on the quality of F-wave extraction. The method in this paper focused on the ECG signals' frequency-domain feature. By analyzing the decomposition results of each layer of the wavelet transform, we got an effective frequency-domain feature and served the frequency-domain feature as one of the bases for detecting AF. This method did not depend on the

extraction of F waves. Simultaneously, our detection results had good accuracy, sensitivity, and specificity.

II. METHODS

A. The processes of analysis

First of all, we removed the high-frequency noise and baseline drift of the ECG signal by filtering. Then the ECG signal was segmented by 5s to detect the R wave peak of each period. In this way, we could extract the mean and variance of the R-R interval, which could identify the degree of regularity of the R-R interval and obtain the time domain characteristics of the ECG signals. Next, the filtered signal was segmented according to R peak to obtain a single-period signal waveform. Then we decomposed the single-period signal waveform by wavelet transform. And we reconstructed the characteristic waveform by the approximate decomposition coefficients of the fourth layer. Furthermore, we obtained the frequency corresponding to the maximum amplitude in the frequency spectrum (MAiFS) by fast Fourier transform of the characteristic waveform. Thus we gained the frequency domain feature of the ECG signals. The above two types of features were used as the finally extracted AF signal features. And using the decision tree classification algorithm to detect AF. Finally, we proved the validity of the extracted frequency-domain features and obtained the accuracy, sensitivity, and specificity of the detection method of AF through the MIT-BIH AF dataset. The processes of the method were shown in Figure 2.

B. Time-domain features extraction method

1)Mathematical morphology filtering

Mathematical morphology [10] is an image analysis discipline based on lattice theory and topology. It is the basic theory of image processing in mathematical morphology. The basic operations include corrosion and expansion.

Let $f(n), (n = 0,1,\dots,N-1)$ and $g(m), (m = 0,1,\dots,M-1)$, among them $N \gg M$. $g(m)$ is the structural element of the morphological filter. The selection of $g(m)$ should be similar to the shape of the preserved waveform and different from the shape of the filtered waveform. To preserve the R-wave and filter out other waveforms, we chose the structural element $g(m) = \{1,1,1\}$.

Defining corrosion operation

$$(f \Theta g)(n) = \min_{m=0,1,\dots,M-1} \{f(n+m) - g(m)\}$$

Defining expansion operation

$$(f \oplus g)(n) = \max_{m=0,1,\dots,M-1} \{f(n-m) + g(m)\}$$

Because of corrosion operation and expansion operation have time sequence, mathematical morphology gives two different morphological operations. Corrosion first followed by expansion is defined as an open operation and expansion first followed by corrosion as a closed operation. Defining $f(n)$ on $g(n)$ open operation

$$f \circ g = (f \Theta g) \oplus g \tag{1}$$

Defining $f(n)$ on $g(n)$ closed operation

$$f \bullet g = (f \oplus g) \Theta g \tag{2}$$

Through mathematical analysis, it can be proved that the morphological opening operation can flatten the peak and the closed operation can fill the trough. For ECG signals, the waveforms except the R wave can be flattened by the mathematical morphology operation.

2)Shannon Energy Envelope

Considering that the ECG signal fluctuates greatly near the R wave and according to the Shannon energy function [11], the response to the low amplitude is weak in the range of (0,1), and the response to the high amplitude is strong. We performed differential and normalization on the filtered signal. Then the resulting function values are smoothly enveloped by a moving average method. The range of (0,1) means the normalized amplitude and is unitless.

$\mathrm{d(n)}$ is the differential of the ECG signal. The Shannon energy operation is defined as

$$y_1(\mathrm{n}) = -|\mathrm{d(n)}|^2 \times \ln(|\mathrm{d(n)}|^2) \tag{3}$$

To prevent signal signature delays during smoothing, we used a sliding mean filter without phase shift

$$\mathrm{y(n)} = \frac{1}{\mathrm{N}}(y_1(\mathrm{n} - \frac{\mathrm{N}-1}{2}) + y_1(\mathrm{n} - \frac{\mathrm{N}-1}{2} + 1) + \cdots + y_1(\mathrm{n} + \frac{\mathrm{N}-1}{2})) \tag{4}$$

If window overflow occurs in the head or tail segment of the signal, making $\min(1, \mathrm{n} - \frac{\mathrm{N}-1}{2})$ and $\max(\mathrm{length(signal)}, \mathrm{n} + \frac{\mathrm{N}-1}{2})$ do some appropriate changes. And the N in the denominator of the formula should be appropriately adjusted. Where L is the length of the signal.

Through the Shannon energy envelope, we obtained the specific position of R peak. Simultaneously, the refractory period is set after each R peak detection. In the refractory period, even if there is a peak in the signal, it is not considered to be an R peak. In this test model, the refractory period was set to 200ms.

C. Frequency domain feature extraction method

Wavelet transform (WT) [12] is a powerful technology for representing a signal in different translations and scales. In practical applications, since the ECG signal is a short-term non-stationary random process, the Fourier transform based on the stationary stochastic process cannot reflect the essential characteristics of AF. The wavelet transform analysis method provides the possibility of extracting non-stationary random signal features.

1) Wavelet transform theory

For any signal $f(t) \in L^2(T)$, the wavelet transform is

$$\mathrm{W_f(a,b)} = < \mathrm{f}, \psi_{\mathrm{a,b}} > = |\mathrm{a}|^{-\frac{1}{2}} \int_{\mathrm{R}} \mathrm{f(t)}\, \overline{\psi(\frac{\mathrm{t}-\mathrm{b}}{\mathrm{a}})}\mathrm{dt} \tag{5}$$

Where $\psi(\mathrm{t})$ is a mother wavelet, a is the dilation factor and b is the translation factor. Different frequency and time localizations can be achieved by adjusting a and b.

Since the ECG signal is stored in the form of discrete finite-length signals, continuous wavelet changes must be discretized for ease of calculation. Usually, the discrete formula of the dilation factor and the translation factor in the continuous wavelet transform is taken as: $\mathrm{a} = \mathrm{a_0^m}$, $\mathrm{b} = \mathrm{na_0^m b_0}$, where $\mathrm{m, n} \in \mathrm{Z}$, $\mathrm{a_0} \neq 1$. The corresponding discrete wavelet function can be expressed as

$$\psi_{\mathrm{m,n}}(\mathrm{t}) = \mathrm{a_0^{-\frac{m}{2}}}\psi(\frac{\mathrm{t}-\mathrm{na_0^m b_0}}{\mathrm{a_0^m}}) = \mathrm{a_0^{-\frac{m}{2}}}\psi(\mathrm{a_0^{-m}t} - \mathrm{nb_0}) \tag{6}$$

At this point, the discrete wavelet transform of $f(t)$ is

$$WT_f(m,n) = \int_R f(t)\,\overline{\psi_{m,n}(t)}dt \tag{7}$$

Its reconstruction formula is

$$f(t) = C\sum_{-\infty}^{\infty}\sum_{-\infty}^{\infty} WT_f(m,n)\,\psi_{m,n}(t) \tag{8}$$

2) Mallat algorithm

Multi-resolution analysis constructs a series of orthogonal function spaces to decompose the sequence into a low-frequency signal and a series of high-frequency signals (the number of high-frequency signals depends on the number of decomposition layers). As for discrete-time signals, the dyadic discrete wavelet transform (DWT) can be implemented by low-pass, h(n), and high-pass, g(n), filters [13]. The Mallat algorithm is a fast algorithm for constructing orthogonal wavelets. The recursive formula of the decomposition can be expressed as

$$CA_{j+1} = H * CA_j$$
$$CD_{j+1} = G * CD_j$$

Where CA_j and CD_j are respectively column vector forms of wavelet coefficients, and H and G are respectively a matrix composed of low-pass filtering and high-pass filter coefficients of the corresponding filter. j is the number of decomposition layers of the wavelet transform.

The signal reconstruction process can be expressed as

$$CA_j = H^* CA_{j+1} + G^* CD_{j+1} \tag{9}$$

It can be seen that the essence of the wavelet transform is a filtering process. The obtained approximate coefficients represent the low-frequency characteristics of the signal, and the detail coefficients represent the high-frequency characteristics of the signal. Through the wavelet transform, we can focus on the frequency characteristics of a certain frequency band of the ECG signal. We decomposed the ECG signal by wavelet, and reconstruct signals by using the data of each frequency band after decomposition. Then we analyzed the frequency domain characteristics of ECG signals by reconstructed signals. Therefore, the wavelet transform can be used to analyze the ECG signal and extract the frequency domain features of AF.

III. RESULTS

A. Data source and preprocessing

The data used in the experiment comes from the MIT-BIH database [4], which is publicly accessible via the web and with ethical approval and consent. The dataset contains 23 annotated ECG records, each of which is approximately 10 hours with a sampling rate of 250Hz and a 12-bit resolution with a range of 10mv. Each record contains ECG1 and ECG2 two signals. In this study, we used ECG1 to do these experiments. The preprocessing was divided into two steps: splitting the signal and filtering. The splitting signal was to divide the input ECG signal into segments of 5 seconds for subsequent processing. Filtering was to design an FIR digital filter by using a window function method and filtering the ECG signal. Its cutoff frequency was set to 0.5Hz and 30Hz. The purpose of setting a cutoff frequency to 30Hz was to eliminate electromyography interference and 50Hz frequency interference. The purpose of setting a cutoff frequency of 0.5Hz was to eliminate human respiration, movement of the electrode and other low-frequency interference. The results were shown in Figure 3.

B. Time-domain feature extraction

As the mean and variance of R-R interval can represent the regularity of ECG signal in different conditions, the mean and variance of R-R interval in sinus rhythm and AF were taken as time-domain features in this paper. The processes can be divided into three steps: mathematical morphological filtering, determining the R-wave position by using the fragrance energy envelope, extracting R-wave waveform and analyzing time-domain features.

Firstly, the preprocessed ECG signal is filtered by mathematical morphology. The result is shown in Figure4.

Then we used Shannon energy calculation for further activation and zero phase shift envelope to extract the envelope curve peak and get R wave position, as shown in Figure5.

After the detection of R waves from sinus rhythm and AF signal segments, we carried on a statistical analysis of mean value, variance and number of R waves of R-R interval. The results were shown in Figure 6.

C. Frequency domain feature extraction

The processes of extracting frequency-domain feature can be divided into three steps: performing four-layer wavelet decomposition, reconstructing based on the fourth layer, performing Fast Fourier Transform and marking the maximum amplitude in the frequency spectrum (MAiFS).

The fourth layer discrete wavelet transform is performed on a single waveform. And we obtained the sub-band signal bandwidth (as shown in Table 1) after decomposition. The sampling frequency is 250Hz.

After using the Fast Fourier transform, the sub-band signals of this waveform were shown in Figure 7 and it could be seen that the frequency distribution of each sub-band signal was consistent with that shown in Table 1.

Table 1 Frequency range of fourth layer discrete wavelet transform

Sub-band	Frequency range (Hz)
CA4	0-7.813
CD4	7.813-15.625
CD3	15.625-31.25
CD2	31.25-62.5
CD1	62.5-125

The table shows the results of the four-layer discrete wavelet transform.

Then we decomposed the AF signal and sinus rhythm signal according to the frequency range of each sub-band. The results were shown in Figure 8 and Figure 9.

Next, we used approximate decomposition coefficients of the fourth layer to reconstruct the sinus rhythm signal and the AF signal. As shown in Figure 10.

Finally, we performed Fast Fourier transform to analyze the two kinds of the reconstructed signals. As shown in Figure 11 and Figure 12.

Thus we obtained the frequency corresponding to the maximum amplitude in the spectrum(MAiFS), which can be used as the frequency domain characteristic of the ECG signals. The statistical results of the frequency-domain feature of sinus rhythm signals and AF signals were shown in Figure 13 (partial data).

D. Classification using decision tree algorithm

The classifier used a decision tree algorithm [14]. Based on the principle of minimizing the Gini index, a decision tree was generated using the CART (classification and regression tree) algorithm. The data obtained from the above experiments were classified using the generated CART decision tree. And the confusion matrix of the classification results was obtained. As shown in Figure 14. From the confusion matrix, we knew that the accuracy of classification reaches 98.9%. Sensitivity(SN) and specificity(SP) are calculated as

$$SE = \frac{TP}{TP+FN} \tag{10}$$

$$SP = \frac{TN}{TN+FP} \tag{11}$$

Where true positive (TP): AF is classified as AF; true negative (TN): sinus rhythm is classified as sinus rhythm; false negative (FN): AF is classified as sinus rhythm; false positive (FP): sinus rhythm is classified as AF. According to the confusion matrix, the sensitivity and specificity of our method were 97.93% and 99.63% respectively. The comparison results were shown in Table 2.

Table 2 Comparison with other conclusions

Method	Sensitivity(SE)	Specificity(SP)
Eric Helfenbein et al [15]	76%	97%
S Dash et al [16]	94%	95%
Tran Thong [17]	89%	91%
Francisco Rinc´on [18]	96%	93%
Proposed algorithm	97.9%	99.6%

The table shows a comparison with other studies about sensitivity and specificity.

IV. Discussion

Through the extraction of the time-domain feature, we found that sinus rhythm signal and AF signal's R-R interval, the mean of R-R interval, the variance of R-R interval and the number of R waves had significant differences. Therefore, these features could be considered as time-domain features in the ECG signal.

Through the extraction of the frequency-domain feature, we found that the frequency corresponding to the maximum amplitude was intensively located in 1Hz in the spectrum of the reconstructed sinus rhythm signal. However, in the spectrum of the reconstructed AF signal, the frequency corresponding to the maximum amplitude was discretely located from 2Hz to 8Hz, which could be regarded as the dominant frequency in ECG signals with AF. Therefore, the frequency corresponding to the maximum amplitude of the spectrum can be used as the frequency-domain feature to detect AF.

Through the decision tree classification algorithm, we classified the sinus rhythm signals and AF signals with high accuracy. Besides, we also got great sensitivity and specificity compared with other studies.

V. Conclusion

The frequency corresponding to the maximum amplitude of the frequency spectrum in the sinus rhythm signal was concentrated and the fluctuation was weak. But the frequency corresponding to the

MAiFS in the atrial fibrillation signal is divergent and irregular. Therefore, the experimental results can prove the validity of the frequency corresponding to MAiFS and the practicability and accuracy of the detection method, which applied this frequency-domain feature. Through the detection method, we obtained good accuracy of classifying sinus rhythm signals and AF signals. And the sensitivity and specificity of our method were pretty good by comparison with other studies.

A. *Abbreviations*

MAiFS: the maximum amplitude in the frequency spectrum.
AF: Atrial fibrillation.
ECG: electrocardiogram

VI. DECLARATIONS

A. *Ethics approval and consent to participate*

Not applicable.

B. *Consent for Publication*

Not applicable.

C. *Availability of data and material*

The MIT-BIH Atrial Fibrillation databases can be found here:
https://www.physionet.org/content/afdb/1.0.0/. Accessed 4th Nov 2000.

D. *Competing interests*

The authors declare that they have no competing interests.

E. *Funding*

This work was partly supported by the Fundamental Research Funds for the Central Universities (N182410001) and supported by the National Training Program of Innovation and Entrepreneurship for Undergraduates (201910145154)

F. *Authors' contributions*

For this paper, YH. and YZ. have equal contributions. Therefore, they are co-first author. JL. supervised the whole project. Hence, JL. is the corresponding author. JP., CZ., and PL. also take part in the project. All authors read and approved the final manuscript.

G. *Acknowledgements*

Not applicable.

REFERENCES

[1] Valentin Fuster, Lars E. Rydén, Davis S. Cannom, Harry J. Crijns, Anne B. Curtis, Kenneth A. Ellenbogen, Jonathan L. Halperin, G. Neal Kay, Jean-Yves Le Huezey, James E. Lowe, S. Bertil Olsson, Eric N. Prystowsky, Juan Luis Tamargo, L. Samuel Wann. 2011 ACCF/AHA/HRS Focused Updates Incorporated Into the ACC/AHA/ESC 2006 Guidelines for the Management of Patients With Atrial Fibrillation[J]. Journal of the American College of Cardiology, 2011, 57(11).

[2] Yong Xia, Naren Wulan, Kuanquan Wang, Henggui Zhang. Detecting atrial fibrillation by deep convolutional neural networks[J]. Computers in Biology and Medicine, 2018, 93.

[3] Kirchhof P, Benussi S, Kotecha D, et al. 2016 ESC Guidelines for the management of atrial fibrillation developed in collaboration with EACTS. [J]. European journal of cardio-thoracic surgery: official journal of the European Association for Cardio-thoracic Surgery,2016,50(5).

[4] Moody GB, Mark RG. A new method for detecting atrial fibrillation using R-R intervals. Computers in Cardiology. 10:227-230 (1983).

[5] Tateno, K., Glass, L. Automatic detection of atrial fibrillation using the coefficient of variation and density histograms of RR and ΔRR intervals. Med. Biol. Eng. Comput. 39, 664–671 (2001).

[6] Maji U, Mitra M, Pal S, et al. Automatic Detection of Atrial Fibrillation Using Empirical Mode Decomposition and Statistical Approach[J]. Procedia Technology, 2013: 45-52.

[7] Paolo Massimo Buscema, Enzo Grossi, Giulia Massini, Marco Breda, Francesca Della Torre. Computer Aided Diagnosis for atrial fibrillation based on new artificial adaptive systems[J]. Computer Methods and Programs in Biomedicine,2020.

[8] He Runnan, Wang Kuanquan, Zhao Na, Liu Yang, Yuan Yongfeng, Li Qince, Zhang Henggui. Automatic Detection of Atrial Fibrillation Based on Continuous Wavelet Transform and 2D Convolutional Neural Networks [J]. Frontiers in physiology, 2018, 9: Article 1206

[9] S. Asgari, A. Mehrnia, M. Moussavi, Automatic detection of atrial fibrillation using stationary wavelet transform and support vector machine, Comput. Biol. Med. (2015) 132–142.

[10] Jian Chen, Hong Chen, Xiaoxia Cai, Pengfei Weng, and Hao Nie "Application of signal processing based on mathematical morphology", Proc. SPIE 10255, Selected Papers of the

Chinese Society for Optical Engineering Conferences held October and November 2016, 102553K (8 March 2017);

[11] Park Jeong-Seon, Lee Sang-Woong, Park Unsang. R Peak Detection Method Using Wavelet Transform and Modified Shannon Energy Envelope[J]. Journal of Healthcare Engineering, 2017:1-14.

[12] Daubechies I. Ten Lectures On Wavelets[J]. The Journal of the Acoustical Society of America, 1992, 93(3): 1671-1671.

[13] Howard L. Resnikoff, Raymond O. WellsJr. Wavelet analysis. Springer-Verlag New York, Inc. 1998.

[14] Alexandre Vallée,, Safar ME, Blacher J. application of a decision tree to establish factors associated with a nomogram of aortic stiffness[J]. Journal of Clinical Hypertension, 2019(7).

[15] Eric Helfenbein, Richard Gregg, James Lindauer, Sophia Zhou, "An Automated Algorithm for the Detection of Atrial Fibrillation in the Presence of Paced Rhythm", Computing in Cardiology 2010; vol 37: pp.113−116.

[16] S Dash, E Raeder, S Merchant, K Chon, "A Statistical Approach for Accurate Detection of Atrial Fibrillation and Flutter", Computers in Cardiology-2009, vol. 36, pp-137−140.

[17] Tran Thong, James McNames, Mateo Aboy, and Brahm Goldstein, "Prediction of Paroxysmal Atrial Fibrillation by Analysis of Atrial Premature Complexes", IEEE transactions on biomedical engineering, Vol. 51, no. 4, pp-561-569, 2004

[18] Francisco Rinc´on, Paolo Roberto Grassi, Nadia Khaled, David Atienza, and Donatella Sciuto, "Automated Real-Time Atrial Fibrillation Detection on a Wearable Wireless Sensor Platform", 34th Annual International Conference of the IEEE EMBS-2012, pp-2472-2475.

VII. FIGURE LEGENDS

(a)

(b)

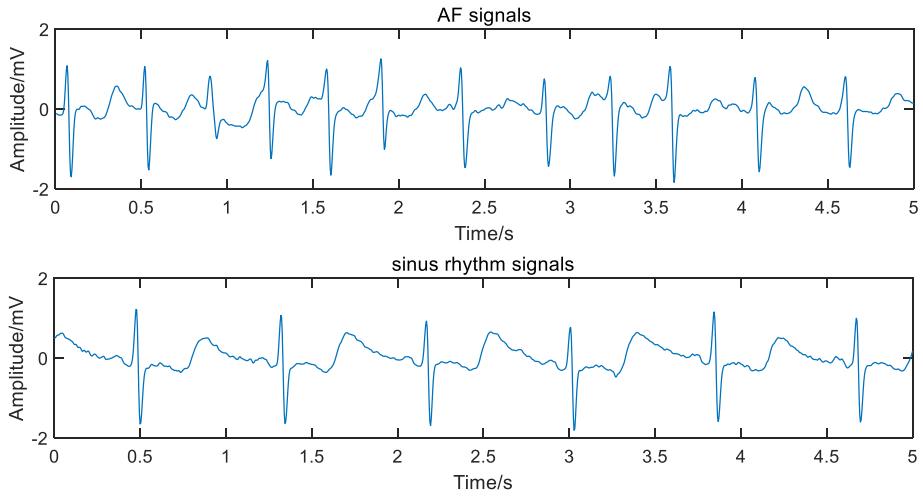

Figure 1 5s original ECG signal in AF(a) and sinus rhythm(b). It can be seen that P waves are replaced by irregular F waves in the AF signals. Other waves are not very different between the AF signal and sinus rhythm signal.

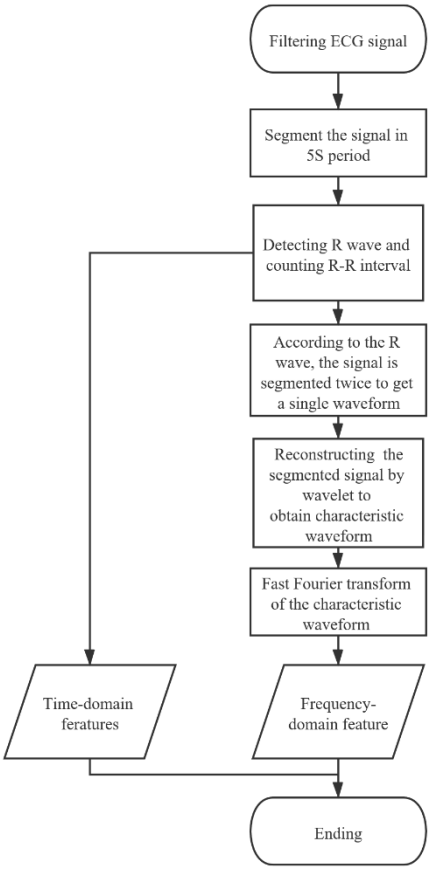

Figure 2 Procedures of extracting features

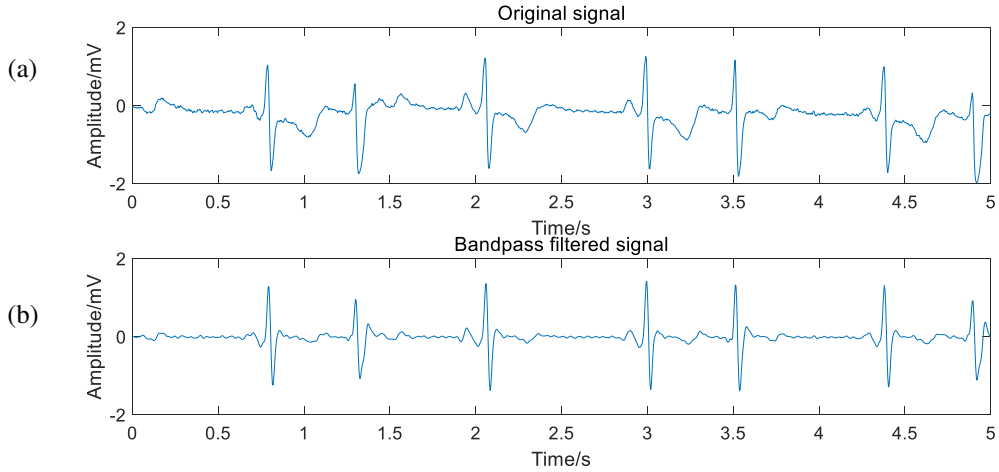

Figure 3 Comparation of original filtered signal and band pass filtered signal. The images show that original signal have some kinds of frequency interference and the band pass filtered signal is more regular than original signal.

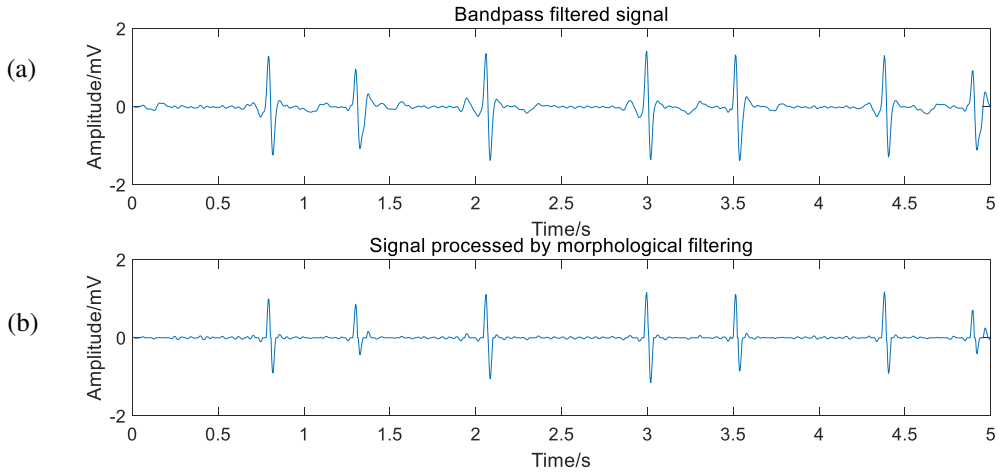

Figure 4 Compare band-pass filtered signal with morphological filtered signal. The image shows that the morphological filter can further eliminate interferences than band-pass filter so that we can obtain the needful signal to do experiments.

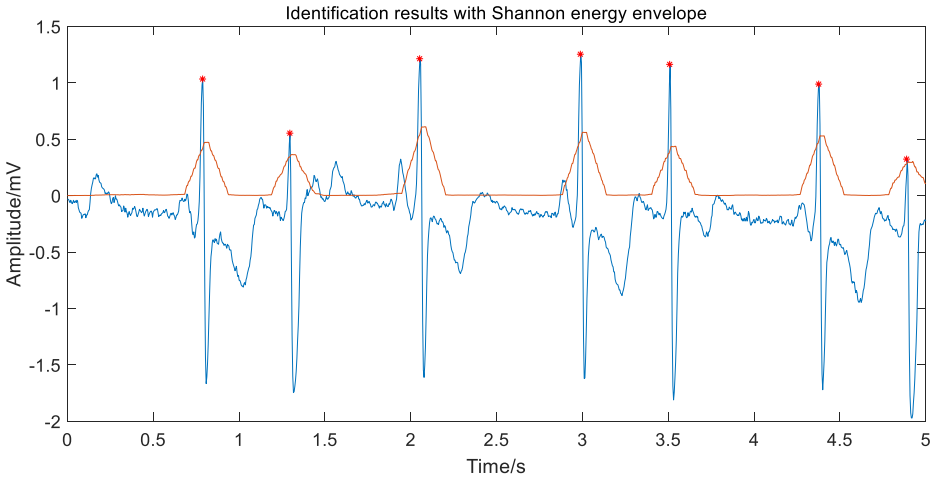

Figure 5 Detecting R wave. The image shows "*" is the result of detection - R peak and indicates the method to be of high accuracy. There is the Shannon energy envelope curve

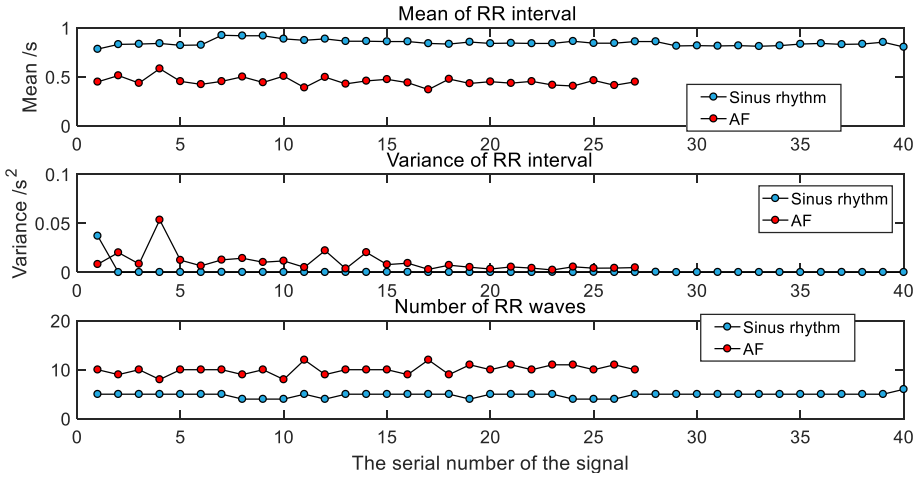

Figure 6 Time-domain features. There are three kinds of features in the image. For the mean of RR interval, sinus rhythm signals were larger than AF signals. For the variance of RR interval, AF ECG signals were a little larger than sinus rhythm signals. For the number of RR intervals, AF signals were more than sinus rhythm signals.

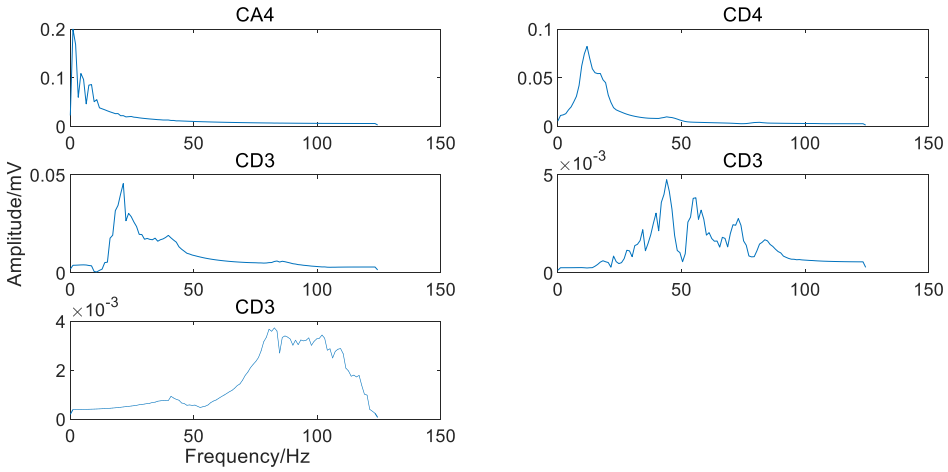

Figure 7 Frequency ranges of sub-band signals. It can be seen that different sub-band has a different spectrum and contains different information in a single waveform.

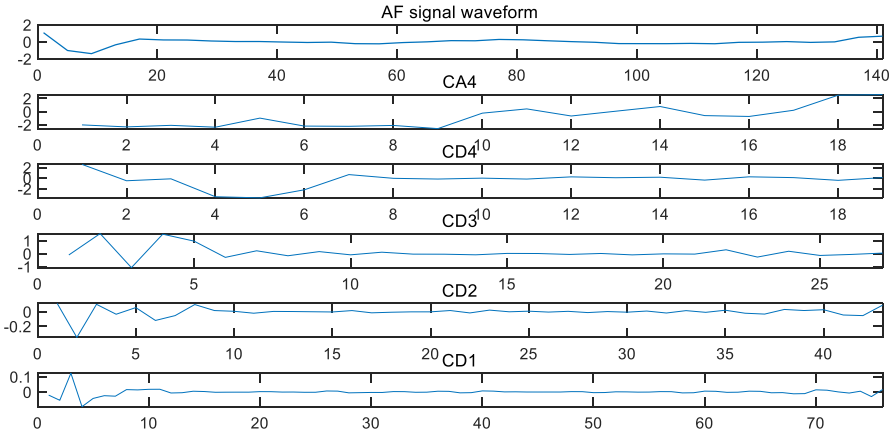

Figure 8 Decomposing single AF signal waveform.

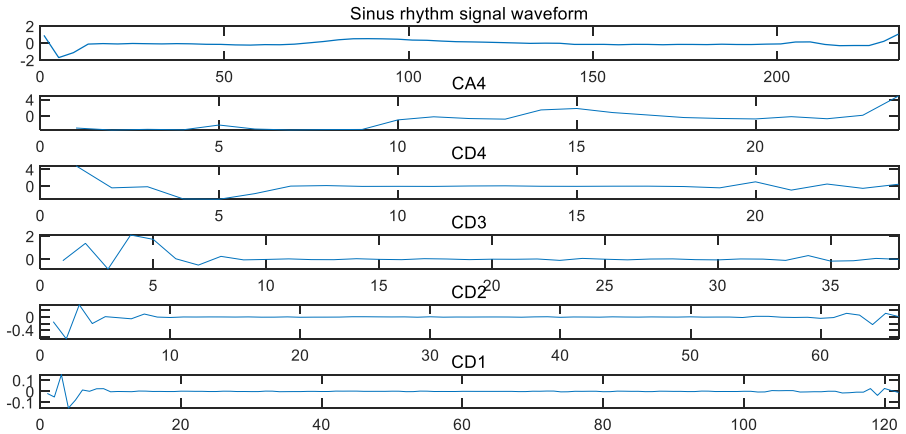

Figure 9 Decomposing single sinus rhythm signal waveform.

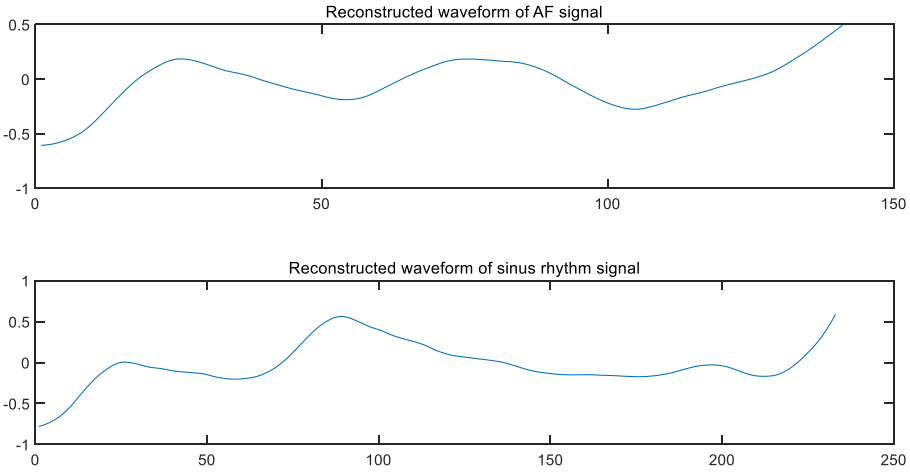

Figure 10 Reconstruction of single AF signal waveform and sinus rhythm signal waveform. The two reconstructed waveforms are largely similar with the extracted single waveforms.

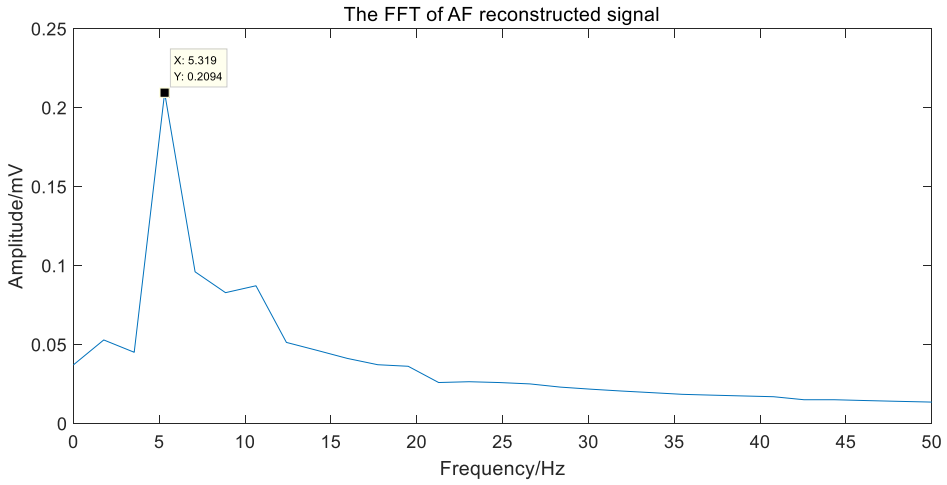

Figure 11 The FFT of AF reconstructed signal.

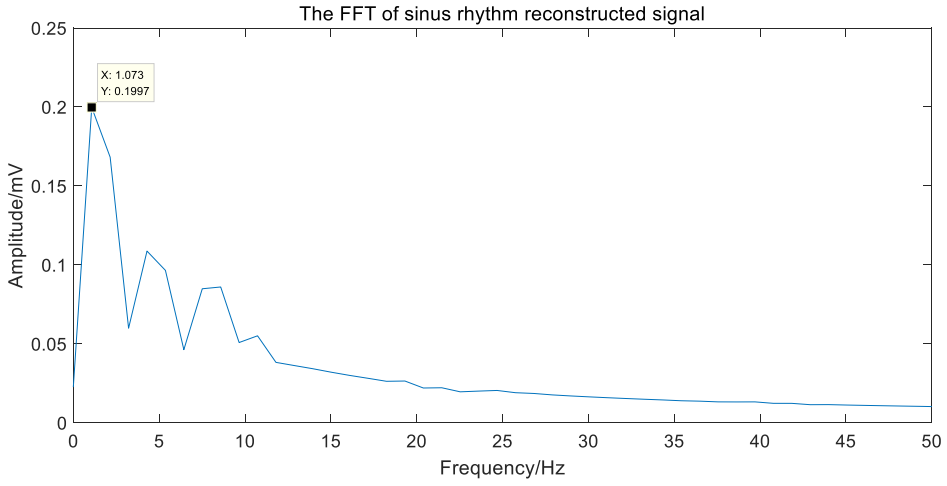

Figure 12 The FFT of sinus rhythm signal.

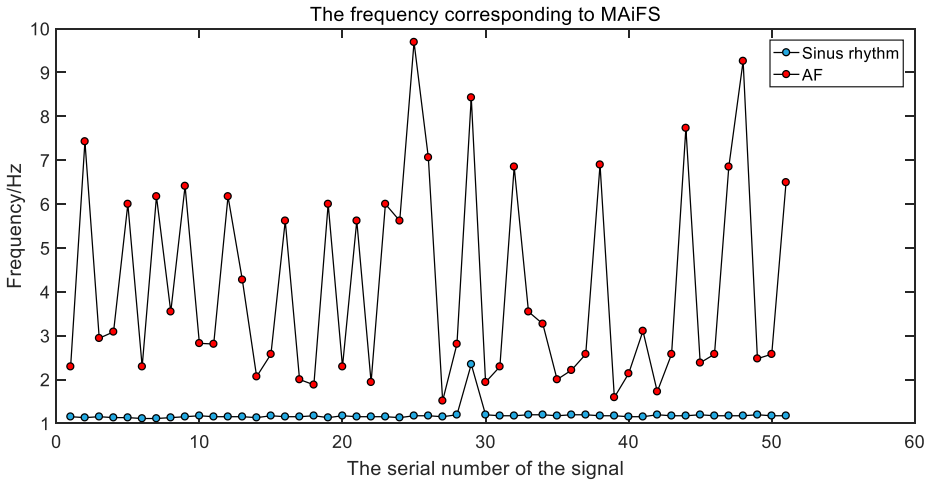

Figure 13 Frequency domain features of AF and sinus rhythm. The frequency-domain feature of AF signals had volatility while sinus rhythm signals had stability.

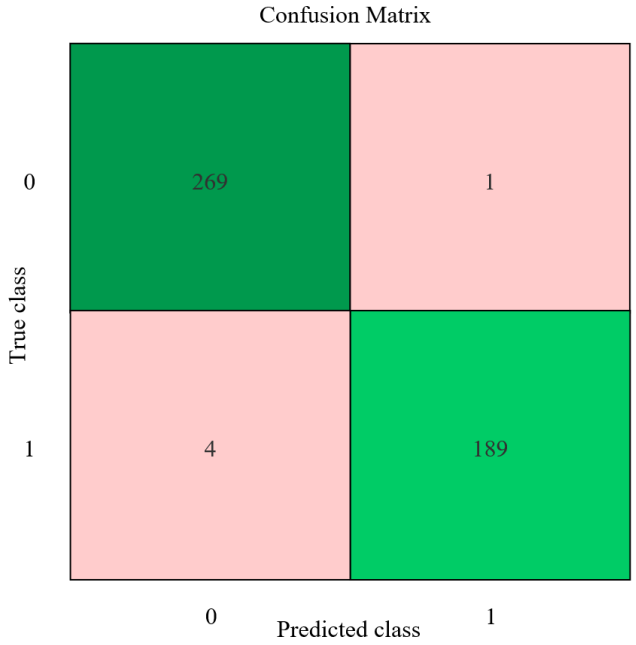

Figure 14 Result of classifying AF signals and sinus rhythm signals. The number in the green rectangle means successful classification and the number in pink rectangle means failed classification.

Figures

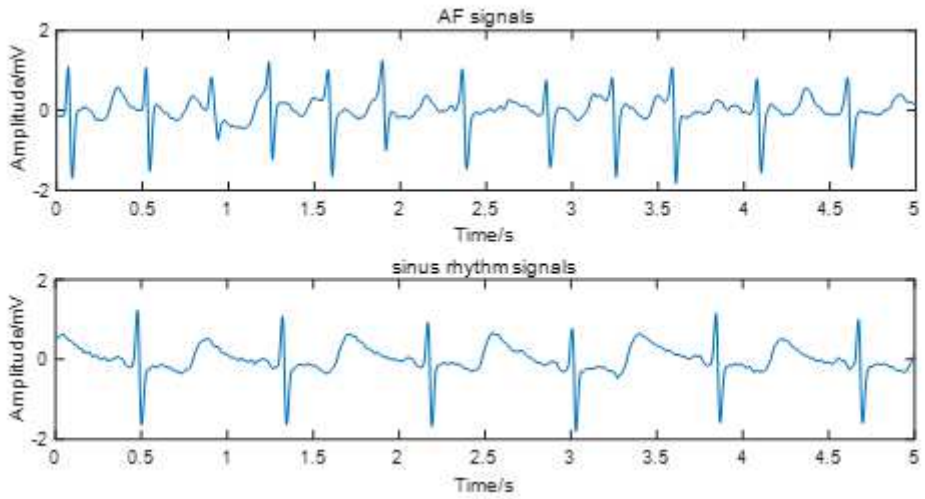

Figure 1

5s original ECG signal in AF(a) and sinus rhythm(b). It can be seen that P waves are replaced by irregular F waves in the AF signals. Other waves are not very different between the AF signal and sinus rhythm signal.

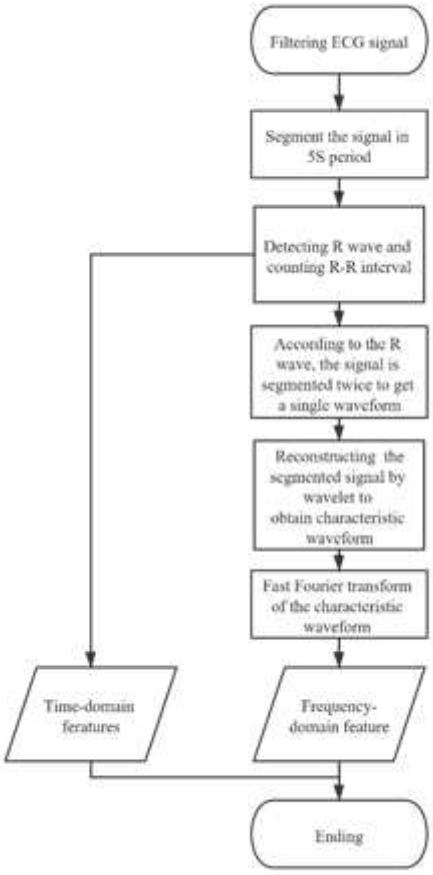

Figure 2

Procedures of extracting features

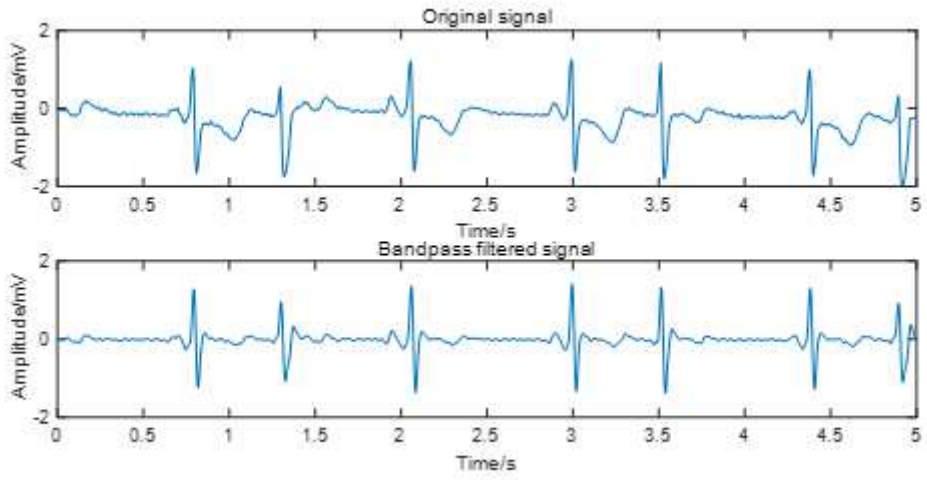

Figure 3

Comparation of original filtered signal and band pass filtered signal. The images show that original signal have some kinds of frequency interference and the band pass filtered signal is more regular than original signal.

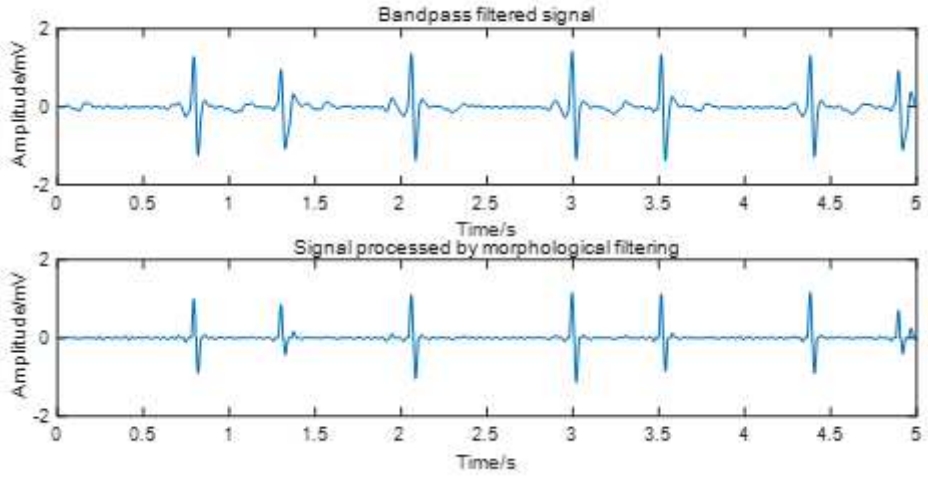

Figure 4

Compare band-pass filtered signal with morphological filtered signal. The image shows that the morphological filter can further eliminate interferences than band-pass filter so that we can obtain the needful signal to do experiments.

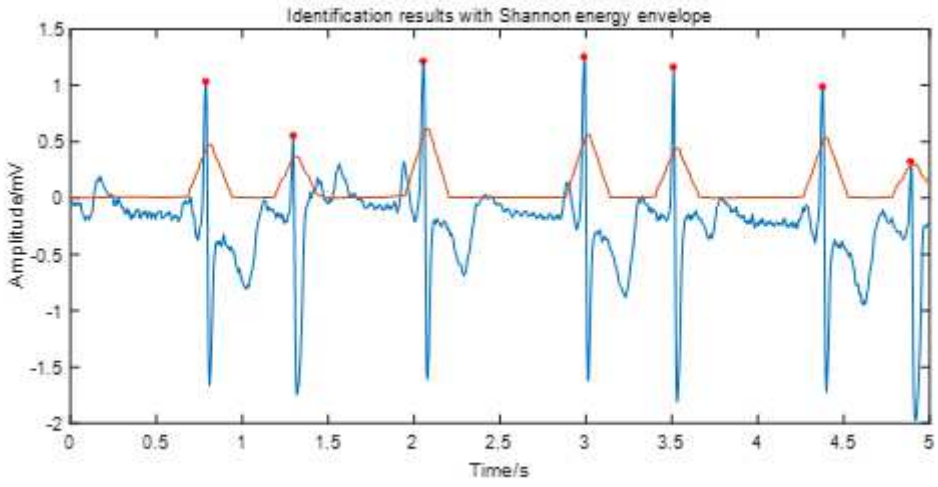

Figure 5

Detecting R wave. The image shows “*” is the result of detection - R peak and indicates the method to be of high accuracy. There is the Shannon energy envelope curve

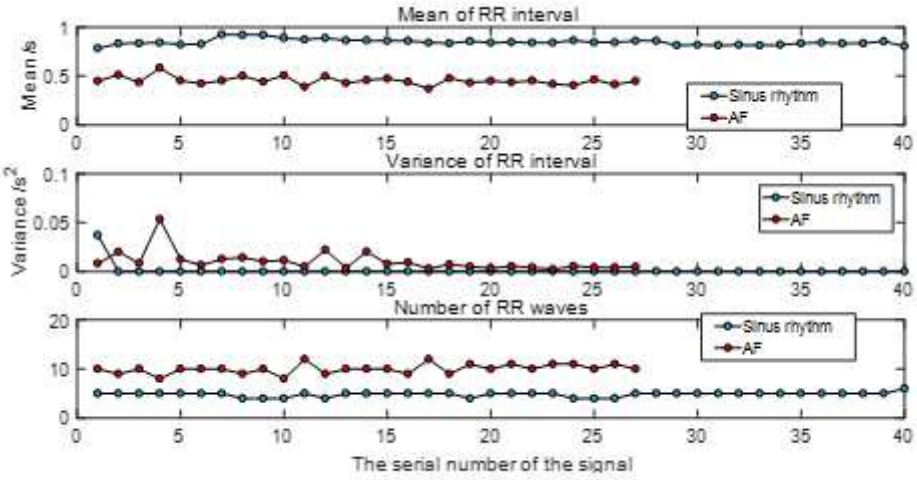

Figure 6

Time-domain features. There are three kinds of features in the image. For the mean of RR interval, sinus rhythm signals were larger than AF signals. For the variance of RR interval, AF ECG signals were a little larger than sinus rhythm signals. For the number of RR intervals, AF signals were more than sinus rhythm signals.

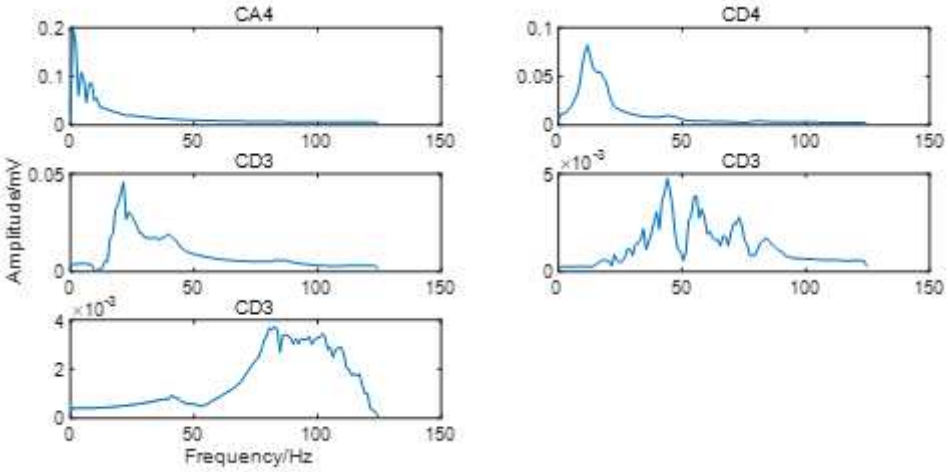

Figure 7

Frequency ranges of sub-band signals. It can be seen that different sub-band has a different spectrum and contains different information in a single waveform.

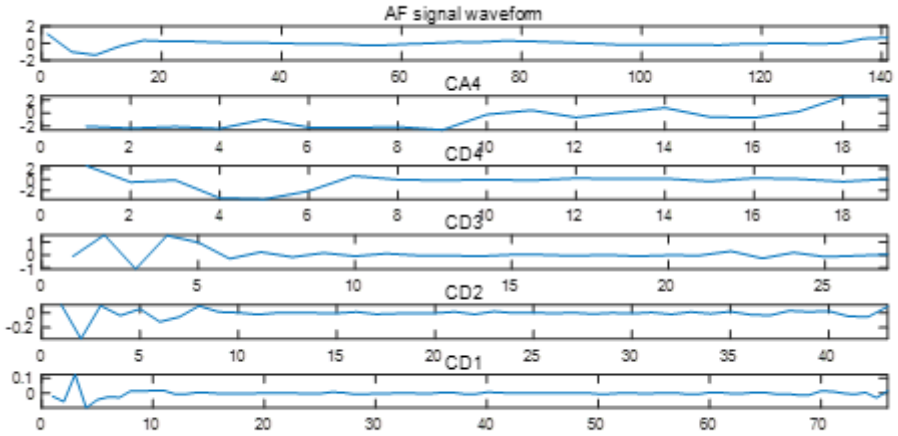

Figure 8

Decomposing single AF signal waveform.

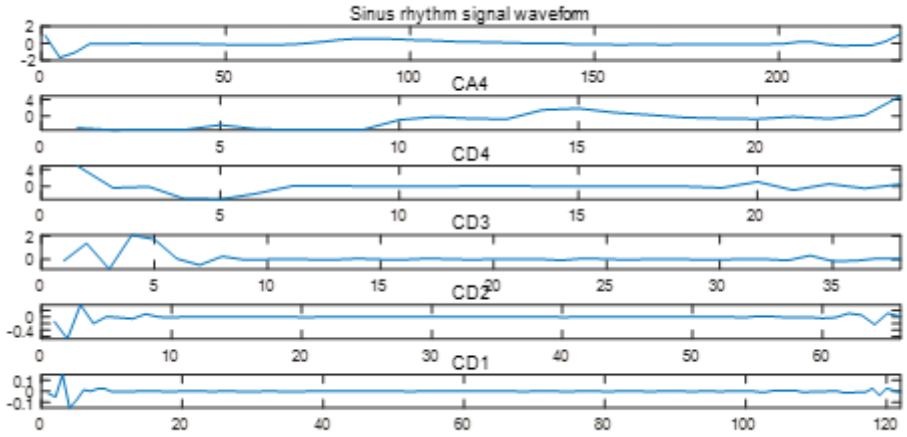

Figure 9

Decomposing single sinus rhythm signal waveform.

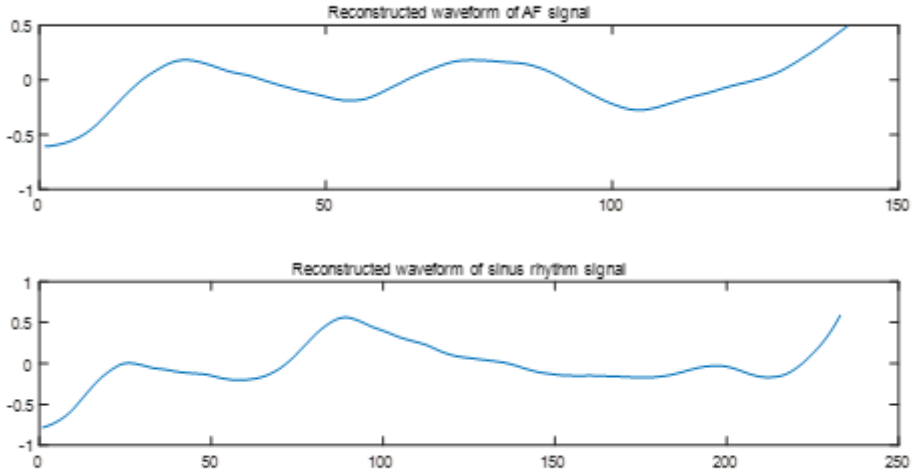

Figure 10

Reconstruction of single AF signal waveform and sinus rhythm signal waveform. The two reconstructed waveforms are largely similar with the extracted single waveforms.

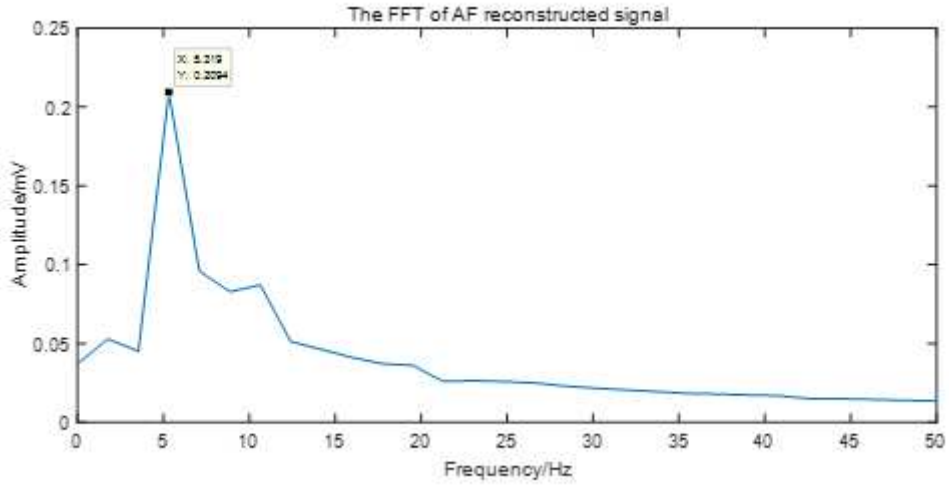

Figure 11

The FFT of AF reconstructed signal.

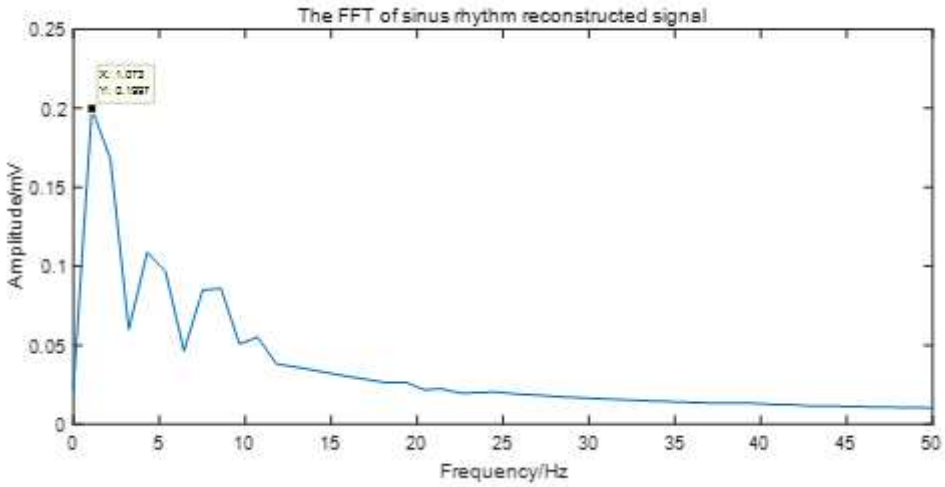

Figure 12

The FFT of sinus rhythm signal.

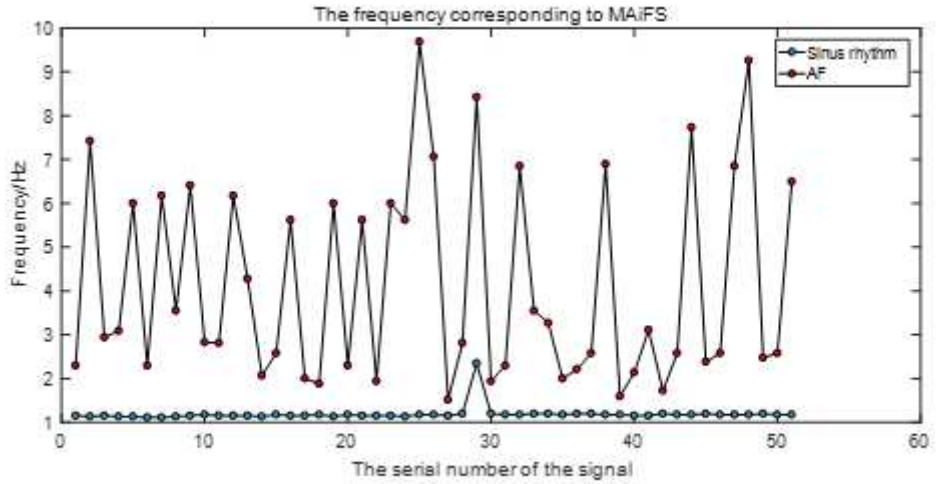

Figure 13

Frequency domain features of AF and sinus rhythm. The frequency-domain feature of AF signals had volatility while sinus rhythm signals had stability.

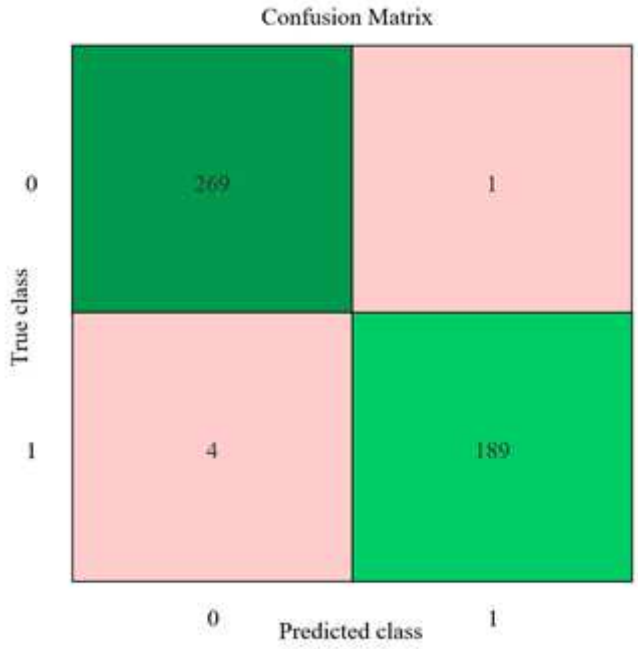

Figure 14

Result of classifying AF signals and sinus rhythm signals. The number in the green rectangle means successful classification and the number in pink rectangle means failed classification.